

Electron–ion interactions in close packed metals

V RAMAMURTHY

Department of Physics, Indian Institute of Technology, New Delhi 110016, India

MS received 1 December 1984; revised 5 February 1985

Abstract. The electron–ion interactions are evaluated exactly over the actual shape of the atomic polyhedron by making use of simple co-ordinate axes transformations and lattice symmetry in the case of hcp and ccp structures. It is shown that the expressions for the interference factor, $S(\mathbf{q}, t)$ of hcp structure are complex while those of ccp structure are real, even when both atomic arrangements are referred to the same orthorhombic co-ordinate axes, and in each case, lattice atom contributions could be distinguished from basis atom contributions to $S(\mathbf{q}, t)$. By comparing these expressions with each other as well as with those obtained by approximating their atomic polyhedra by an ellipsoid of equivalent volume, apparent differences between interference factors of hcp and ccp structures, validity of Wigner–Seitz approximation for a diatomic lattice and the manner in which the electron–ion interactions contribute to the different modes of vibration in a hexagonal lattice are discussed.

Keywords. Electron–ion interaction; interference factor; coordinate axes transformation; umklapp process; hcp lattice; ccp lattice.

PACS No. 63-20

1. Introduction

The electron–ion interactions manifest themselves whenever the thermal motion of the ion perturbs the energies of conduction electrons. It is necessary to evaluate the former by averaging the latter over the actual shape of the atomic polyhedron in order to ensure that the form factors and the interference factor, $S(\mathbf{q})$ so obtained are sensitive to the symmetry of the lattice. Ramamurthy (1978, hereinafter referred to as I) has shown that this sum could be evaluated exactly in the case of cubic structures as well as tetragonal structures (Ramamurthy 1979) by exploiting their lattice symmetry and in each case there are several alternative (but equivalent) ways of writing down the interference factor, $S(\mathbf{q})$. Besides, one or the other of these expressions was obtained by Bross and Bohn (1967), Sharan *et al* (1972, 1973) and Ashokkumar (1973). On the contrary, no attempt has been made so far to deduce equivalent expressions for $S(\mathbf{q})$ in the case of hexagonal close-packed (hcp) structures and to compare them with the corresponding expressions, published elsewhere, in the case of cubic close-packed (ccp) structures. Since the amplitude of thermal motion of a lattice atom differs from that of a basis atom in a diatomic lattice, it is all the more important to distinguish between their contributions to $S(\mathbf{q})$ as well as to determine the manner in which the umklapp processes contribute and restore the translational symmetry to the optical modes of vibration. Hence, the present paper describes an exact evaluation of the interference factors associated with the close packed structures which makes use of their lattice

symmetry. To facilitate the comparison between these structures and their interference factors, the atomic arrangements in both cases are referred to orthorhombic coordinate axes.

2. Theory

When the effect of thermal motion of the ion, represented by the wave vector, \mathbf{q} is averaged over the conduction electrons present in the atomic polyhedron without approximating it by a sphere or an ellipsoid of equivalent volume, but treating the electrons as free (the band structure effects and the exchange as well as the correlation effects being taken into account through appropriate effective mass and screening function (Ramamurthy and Singh 1978), respectively the interference factor, $S(\mathbf{q})$ is given by

$$S(\mathbf{q}) = \int_{\Omega} \exp(i\mathbf{q} \cdot \mathbf{r}) d\Omega/\Omega, \quad (1)$$

where Ω is the volume of the atomic polyhedron. This expression could be reduced, by making use of Gauss' divergence theorem and some vector identities involving ∇ (see equation (2) in I), to the following forms:

$$S_2(\mathbf{q}) = \frac{(\sigma_x + \sigma_y + \sigma_z)}{\Omega(q_x + q_y + q_z)}, \quad (2a)$$

$$S_3(\mathbf{q}) = \frac{(q_x\sigma_x + q_y\sigma_y + q_z\sigma_z)}{\Omega(q_x^2 + q_y^2 + q_z^2)}. \quad (2b)$$

Here σ_x , σ_y and σ_z are the Cartesian components of σ defined by

$$\sigma = \frac{1}{i} \int_{\mathbf{s}} \exp(i\mathbf{q} \cdot \mathbf{r}) d\mathbf{S}, \quad (3)$$

where the integration is over the surface of the atomic polyhedron and hence has to be evaluated separately for each atomic arrangement. This integral is evaluated by adopting the procedure described in I in the case of diatomic hcp and triatomic ccp structures in the next section.

3. Evaluation of the interference factors

3.1 hcp structure

The atomic polyhedron of hcp arrangement is shown in figure 1(a). It is a dodecahedron consisting of three pairs of isosceles trapezoidal faces, denoted by (200), (110) and $(1\bar{1}0)$, parallel to the z axis and three pairs of rhombic faces, denoted by $(1\bar{1}1)$, $(\bar{1}\bar{1}1)$ and (021), which intersect the z axis at $\pm(3c^2 + 4a^2)/6c$ where $2a$ and $2c$ are the lattice constants along x and z directions. The former has one side of length $2a(1 + 3t^2)^{1/2}/3t$ with $t = c/a$ common with the latter. All faces, except a pair of (021) rhombic faces contribute to σ_x , a pair of (200) trapezoidal faces do not contribute to σ_y , whereas none of the trapezoidal faces contribute to σ_z . Nevertheless, the symmetry associated with the polyhedron reduces the evaluation of the integral (3) to that of contributions from trapezoidal and rhombic faces to σ_x and σ_z , respectively. Since the (200) trapezoidal faces are

perpendicular to the x axis, their contribution to σ_x could be expressed as

$$\sigma_x(200) = \left[\frac{\exp(iq_x x)}{i} \right]_{-a}^a \int_{-a/t_1}^{a/t_1} \int_{-d}^d \exp(iq_y y) \exp(iq_z z) dS_x, \tag{4}$$

where $t_1 = \sqrt{3}$ and $d = (3c^2 - 2a^2)/6c$. Besides, the co-ordinate axes transformation

$$X = \cos \phi (x + t_1 y), Y = \sin \phi (y/t_1 - x) \text{ and } Z = z, \tag{5}$$

which rotates x and y axes through an angle $\phi = \tan^{-1}(t_1) = 60^\circ$ about the Z axis and orients the (110) trapezoidal faces perpendicular to the X axis, is made use of to write down their contribution to σ_x in the form

$$\sigma_x(110) = \left[\frac{\exp\{i(q_x + t_1 q_y)X\}}{i} \right]_{-a/2}^{a/2} \int_{-a/2}^{a/2} \int_{-d}^d \exp\{i(q_y/t_1 - q_x)Y\} \exp(iq_z Z) dS_x. \tag{6}$$

The evaluation of these integrals yields

$$\sigma_x(200) = \frac{4 \sin(q_x a)}{iq_z} \left\{ \sin[(q_y + q_z/s)a'] \exp(iq_z d)/(q_y + q_z/s) - \sin[(q_y - q_z/s)a'] \exp(-iq_z d)/(q_y - q_z/s) \right\} \tag{7}$$

and

$$\sigma_x(110) = \frac{4 \sin[(q_x + t_1 q_y)a/2]}{iq_z} \left\{ \frac{\sin[(t_1 q_x - q_y + q_z/\gamma)a'/2] \exp(iq_z d)}{(t_1 q_x - q_y + q_z/\gamma)} - \frac{\sin[(t_1 q_x - q_y - q_z/\gamma)a'/2] \exp(-iq_z d)}{(t_1 q_x - q_y - q_z/\gamma)} \right\}, \tag{8}$$

with $a' = a/t_1$, $s = t_1 t$ and $\gamma = t_1 t/2$. The corresponding contribution from (110) trapezoidal faces could easily be written, by substituting $-q_y$ for q_y in the complex conjugate of (8), as

$$\sigma_x(1\bar{1}0) = \frac{4 \sin[(q_x - t_1 q_y)a/2]}{iq_z} \left\{ \frac{\sin[(t_1 q_x + q_y - q_z/\gamma)a'/2] \exp(iq_z d)}{(t_1 q_x + q_y - q_z/\gamma)} - \frac{\sin[(t_1 q_x + q_y + q_z/\gamma)a'/2] \exp(-iq_z d)}{(t_1 q_x + q_y + q_z/\gamma)} \right\}. \tag{9}$$

Further, the co-ordinate axes transformation

$$Z = \frac{t_1}{(4 + 3t^2)^{1/2}} [tz + x - y/t_1], \chi = \frac{[x + t_1 y]}{\sqrt{2}} \text{ and } \eta = \frac{3t}{[2(4 + 3t^2)]^{1/2}} [\frac{4}{3}z/t - x + y/t_1], \tag{10}$$

orients the (111) rhombic face perpendicular to the Z axis and transforms it into a square. Hence its contribution to σ_z could be expressed as

$$\sigma_z(1\bar{1}1) = \left[\frac{\exp\{i(tq_z + q_x - q_y/t_1)Z\}}{i} \right]^{a/2} \int_{-a/2}^{a/2} \int_{-a/2}^{a/2} \exp\{i(q_x + t_1 q_y)\chi\} \exp\{i(\frac{4}{3}q_z/t - q_x + q_y/t_1)\eta\} dS_z. \tag{11}$$

Making use of the co-ordinate axes transformation

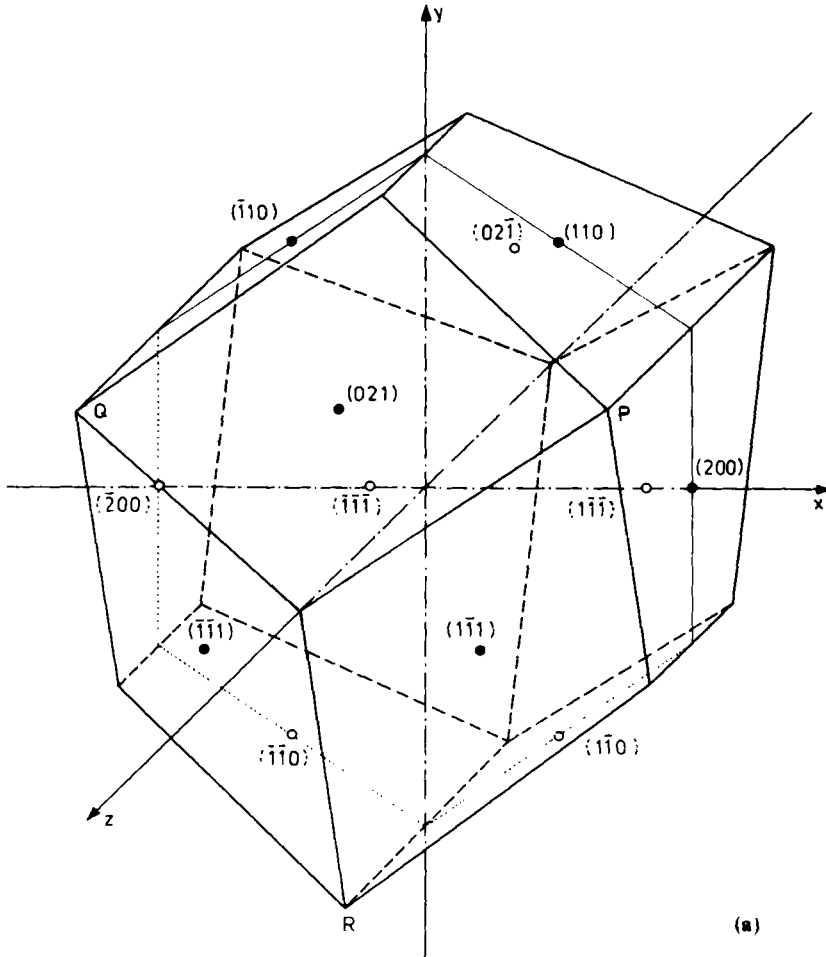
$$Z = Z, \quad X = \frac{1}{2}(\chi + \eta) \text{ and } Y = \frac{1}{2}(\eta - \chi), \tag{12}$$

which rotates χ and η axes through 45° about the Z axis, the integral is evaluated to obtain

$$\begin{aligned} \sigma_z(1\bar{1}\bar{1}) &= 8t_1 \sin [(q_z/\gamma - t_1 q_x - q_y)a'/2] \sin [(q_z/\gamma + 2q_y)a'/2] \\ &\quad \exp [i(tq_z + q_x - q_y/t_1)a/2] / i(q_z/\gamma - t_1 q_x - q_y) (q_z/\gamma + 2q_y). \end{aligned} \tag{13}$$

The corresponding contributions from $(1\bar{1}\bar{1})$, $(\bar{1}\bar{1}1)$ and $(\bar{1}\bar{1}\bar{1})$ rhombic faces could be written as follows by replacing q_z by $-q_z$, q_x by $-q_x$ and q_z, q_x by $-q_z, -q_x$ respectively in (13):

$$\begin{aligned} \sigma_z(1\bar{1}\bar{1}) &= 8t_1 \sin [(q_z/\gamma + t_1 q_x + q_y)a'/2] \sin [(q_z/\gamma - 2q_y)a'/2] \\ &\quad \exp [-i(tq_z - q_x + q_y/t_1)a/2] / i(q_z/\gamma + t_1 q_x + q_y) (q_z/\gamma - 2q_y), \end{aligned} \tag{14}$$



(a)

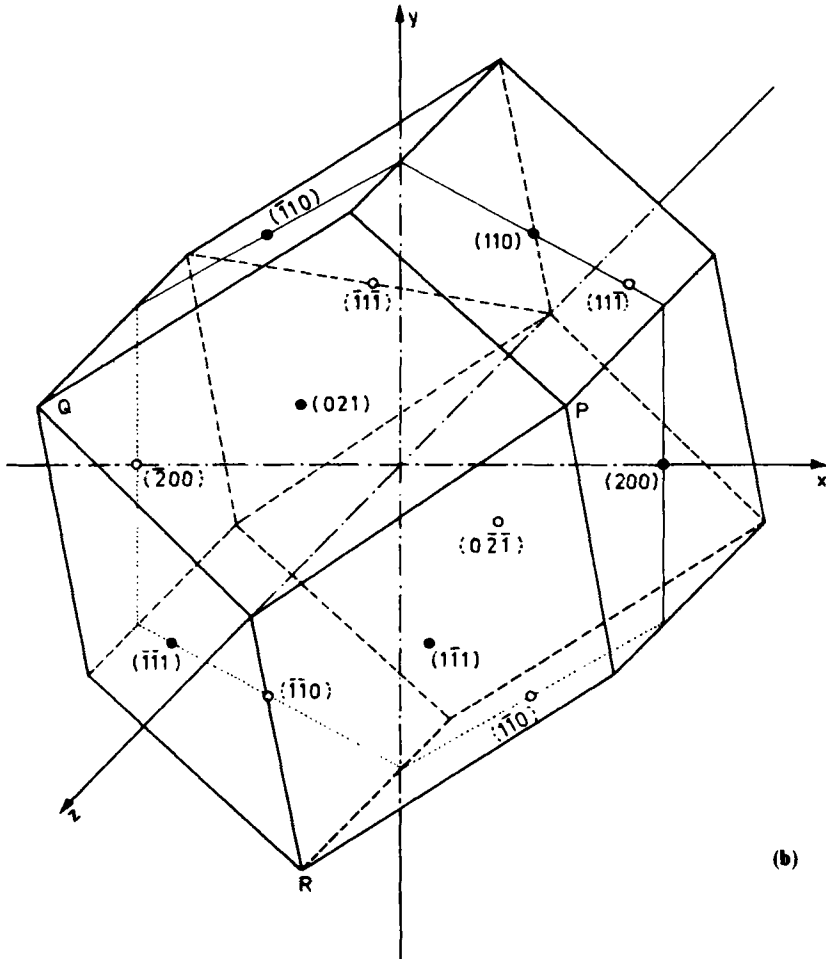


Figure 1. Atomic polyhedra of close packed metals referred to orthorhombic coordinate axes: (a) hcp structure (b) ccp structure. ●, ○ and triple integers denote the centre and Miller indices of each face. The cubic coordinate axes pass through $P(a, a/\sqrt{3}, c/2)$, $Q(-a, a/\sqrt{3}, c/2)$ and $R(0, -2a/\sqrt{3}, c/2)$.

$$\sigma_z(\bar{1}\bar{1}\bar{1}) = 8t_1 \sin [(q_z/\gamma + t_1 q_x - q_y)a'/2] \sin [(q_z/\gamma + 2q_y)a'/2] \exp [i(tq_z - q_x - q_y/t_1)a/2] / i(q_z/\gamma + t_1 q_x - q_y) (q_z/\gamma + 2q_y) \quad (15)$$

and

$$\sigma_z(\bar{1}\bar{1}\bar{1}) = 8t_1 \sin [(q_z/\gamma - t_1 q_x + q_y)a'/2] \sin [(q_z/\gamma - 2q_y)a'/2] \exp [-i(tq_z + q_x + q_y/t_1)a/2] / i(q_z/\gamma - t_1 q_x + q_y) (q_z/\gamma - 2q_y). \quad (16)$$

On the other hand, the co-ordinate axes transformation

$$Z = \sin \theta(\gamma z + y), \quad x = x \quad \text{and} \quad \eta = \cos \theta(y - z/\gamma), \quad (17)$$

rotates the z and y axes through an angle $\theta = \tan^{-1}(1/\gamma)$ about the x axis and orients the (021) rhombic face perpendicular to the Z axis. Its contribution to σ_z is therefore given

by

$$\sigma_z(021) = \left[\frac{\exp \{i(\gamma q_z + q_y)Z\}}{i} \right]_{-a}^{a'} \int_{-a}^a \int_{-a'}^{a'} \exp(iq_x x) \exp \{i(q_y - q_z/\gamma)\eta\} dS_z. \quad (18)$$

This integral is evaluated with the help of the co-ordinate axes transformation

$$\mathbf{X} = \frac{1}{2}(\mathbf{x} + t_1\boldsymbol{\eta}), \quad \mathbf{Y} = \frac{1}{2}(\boldsymbol{\eta}/t_1 - \mathbf{x}) \quad \text{and} \quad \mathbf{Z} = \mathbf{Z}, \quad (19)$$

which transforms the rhombic face into a square face and rotates x and η axes through 45° about the Z axis, to arrive at the expression

$$\sigma_z(021) = 8t_1 \sin [(q_z/\gamma - q_y + t_1q_x)\alpha'/2] \sin [(q_z/\gamma - q_y - t_1q_x)\alpha'/2] \exp [i(\gamma q_z + q_y)\alpha'] / i \{ (q_z/\gamma - q_y)^2 - (t_1q_x)^2 \}. \quad (20)$$

The corresponding contribution from $(02\bar{1})$ rhombic face could be written down, by substituting $-q_z$ for q_z in (20), as

$$\sigma_z(02\bar{1}) = 8t_1 \sin [(q_z/\gamma + q_y - t_1q_x)\alpha'/2] \sin [(q_z/\gamma + q_y + t_1q_x)\alpha'/2] \exp [-i(\gamma q_z - q_y)\alpha'] / i \{ (q_z/\gamma + q_y)^2 - (t_1q_x)^2 \}. \quad (21)$$

Similar expressions for the contributions from (111) rhombic faces and from all faces, except (200) trapezoidal faces, to σ_x and σ_y respectively, are obtained by taking into account the corresponding components of area of these faces. For instance, x and y components are t^{-1} and s^{-1} times the z component of area of (111) rhombic faces and hence their contributions to the former and the latter are related by

$$\begin{aligned} & \sigma_x(1\bar{1}1) + \sigma_x(1\bar{1}\bar{1}) + \sigma_x(\bar{1}\bar{1}1) + \sigma_x(\bar{1}\bar{1}\bar{1}) \\ &= \left[\frac{\sigma_z(1\bar{1}1) - \sigma_z(1\bar{1}\bar{1}) - \sigma_z(\bar{1}\bar{1}1) + \sigma_z(\bar{1}\bar{1}\bar{1})}{t} \right]. \end{aligned} \quad (22)$$

and

$$\begin{aligned} & \sigma_y(1\bar{1}1) + \sigma_y(1\bar{1}\bar{1}) + \sigma_y(\bar{1}\bar{1}1) + \sigma_y(\bar{1}\bar{1}\bar{1}) \\ &= \left[\frac{-\sigma_z(1\bar{1}1) + \sigma_z(1\bar{1}\bar{1}) - \sigma_z(\bar{1}\bar{1}1) + \sigma_z(\bar{1}\bar{1}\bar{1})}{s} \right]. \end{aligned} \quad (23)$$

On the contrary, y component is γ^{-1} times the z component of area of (021) rhombic faces while it is t_1 times the x component of area of (110) trapezoidal faces and their contributions to σ_y are therefore given by

$$\sigma_y(021) + \sigma_y(02\bar{1}) = [\sigma_z(021) - \sigma_z(02\bar{1})]/\gamma \quad (24)$$

and

$$\sigma_y(110) + \sigma_y(1\bar{1}0) = t_1[\sigma_x(110) - \sigma_x(1\bar{1}0)]. \quad (25)$$

3.2 ccp structure

The atomic polyhedron of ccp arrangement is shown in figure 1(b). It is a dodecahedron consisting of three pairs of parallelogram faces, denoted by (200) , (110) and $(1\bar{1}0)$, parallel to the z axis and three pairs of rhombic faces, denoted by $(1\bar{1}1)$, $(\bar{1}\bar{1}1)$ and (021) which intersect the z axis at $\pm (3c^2 + 4a^2)/6c$ where $2a$ and $3c$ are the lattice constants along the x and z directions. The former has one side of length $2a(1 + 3t^2)^{1/2}/3t$ with

$t = c/a$, common with the latter. All faces, except a pair of (021) rhombic faces contribute to σ_x , a pair of (200) parallelogram faces do not contribute to σ_y while only the rhombic faces contribute to σ_z . However, the symmetry associated with the polyhedron reduces the evaluation of the integral (3) to that of contributions to σ_x and σ_z from parallelogram and rhombic faces, respectively. The contribution to σ_x from the (200) parallelogram faces which are perpendicular to the x axis, could be written as

$$\sigma_x(200) = \left[\frac{\exp(iq_x x)}{i} \right]_{-a}^a \int_{-a'}^{a'} \int_{-d}^d \exp(iq_y y) \exp(iq_z z) dS_x \quad (26)$$

whereas that from the (110) parallelogram faces could be expressed using the co-ordinate axes transformation (5) in the form

$$\sigma_x(110) = \left[\frac{\exp\{i(q_x + t_1 q_y)X\}}{i} \right]_{-a/2}^{a/2} \int_{-a/2}^{a/2} \int_{-d}^d \exp\{i(q_y/t_1 - q_x)Y\} \exp(iq_z Z) dS_X. \quad (27)$$

The evaluation of these integrals yields

$$\sigma_x(200) = \frac{8 \sin(q_x a) \sin[(q_y + q_z/s)a'] \sin(q_z d)}{q_x(q_y + q_z/s)} \quad (28)$$

and

$$\sigma_x(110) = \frac{8 \sin[(q_x + t_1 q_y)/a/2] \sin[(t_1 q_x - q_y + q_z/\gamma)a'/2] \sin(q_z d)}{q_x(t_1 q_x - q_y + q_z/\gamma)}. \quad (29)$$

The corresponding contribution from (1 $\bar{1}$ 0) parallelogram faces could be written as follows by replacing q_y, q_z by $-q_y, -q_z$ in (29):

$$\sigma_x(1\bar{1}0) = \frac{8 \sin[(q_x - t_1 q_y)a/2] \sin[(t_1 q_x + q_y - q_z/\gamma)a'/2] \sin(q_z d)}{q_x(t_1 q_x + q_y - q_z/\gamma)}. \quad (30)$$

In addition, since the co-ordinate axes transformation (10) transforms the (1 $\bar{1}$ 1) rhombic faces into square faces and orients them perpendicular to the Z axis, their contribution to σ_z could be written in the form

$$\sigma_z(1\bar{1}1) = \left[\frac{\exp\{i(tq_z + q_x - q_y/t_1)Z\}}{i} \right]_{-a/2}^{a/2} \int_{-a/2}^{a/2} \int_{-a/2}^{a/2} \exp\{i(q_x + t_1 q_y)\chi\} \exp\{i(\frac{2}{3}q_z/t - q_x + q_y/t_1)\eta\} dS_Z. \quad (31)$$

The evaluation of this integral, by making use of the co-ordinate axes transformation (12) which rotates χ and η axes through 45° about the Z axis, yields

$$\sigma_z(1\bar{1}1) = \frac{16t_1 \sin[(tq_z + q_x - q_y/t_1)a/2] \sin[(q_z/\gamma - t_1 q_x - q_y)a'/2] \sin[(q_z/\gamma + 2q_y)a'/2]}{(q_z/\gamma - t_1 q_x - q_y)(q_z/\gamma + 2q_y)}. \quad (32)$$

The corresponding contribution from ($\bar{1}$ 11) rhombic faces could be written, by substituting $-q_x$ for q_x in (32), as

$$\sigma_z(\bar{1}11) = \frac{16t_1 \sin[(tq_z - q_x - q_y/t_1)a/2] \sin[(q_z/\gamma + t_1 q_x - q_y)a'/2] \sin[(q_z/\gamma + 2q_y)a'/2]}{(q_z/\gamma + t_1 q_x - q_y)(q_z/\gamma + 2q_y)}. \quad (33)$$

On the contrary, the co-ordinate axes transformation (17) rotates the z and y axes through an angle $\theta = \tan^{-1}(1/\gamma)$ about the x axis and orients the (021) rhombic faces perpendicular to the Z axis. Hence their contribution to σ_z is given by

$$\sigma_z(021) = \left[\frac{\exp\{i(\gamma q_z + q_y)Z\}}{i} \right]_{-a'}^{a'} \int_{-a'}^a \int_{-a'}^{a'} \exp(iq_x x) \exp\{i(q_y - q_z/\gamma)\eta\} dS_z. \quad (34)$$

By means of the co-ordinate axes transformation (19) which transforms these rhombic faces into square faces and rotates the x and η axes through 45° about the Z axis, the integral is evaluated to obtain

$$\sigma_z(021) = \frac{16t_1 \sin[(\gamma q_z + q_y)a'] \sin[(q_z/\gamma - q_y + t_1 q_x)a'/2] \sin[(q_z/\gamma - q_y - t_1 q_x)a'/2]}{[(q_z/\gamma - q_y)^2 - (t_1 q_x)^2]}. \quad (35)$$

Similar expressions for the contributions to σ_x from (111) rhombic faces and to σ_y from all faces except the (200) parallelogram faces are obtained by taking into consideration the differences in the corresponding components of area of these faces. For example, z component is t times and s times the x and y components of area of (111) rhombic faces, respectively and hence their contributions to the latter are given by

$$\sigma_x(1\bar{1}1) + \sigma_x(\bar{1}11) = [\sigma_x(1\bar{1}1) - \sigma_x(\bar{1}11)]/t \quad (36)$$

and

$$\sigma_y(1\bar{1}1) + \sigma_y(\bar{1}11) = -[\sigma_x(1\bar{1}1) + \sigma_x(\bar{1}11)]/s. \quad (37)$$

On the other hand, the z component of area of (021) rhombic faces is γ times its y component while the y component of area of (110) parallelogram faces is t_1 times its x component and hence their contributions to σ_y are given by

$$\sigma_y(021) = \sigma_z(021)/\gamma \quad (38)$$

and

$$\sigma_y(110) + \sigma_y(1\bar{1}0) = t_1[\sigma_x(110) - \sigma_x(1\bar{1}0)]. \quad (39)$$

3.3 Expressions for $S(\mathbf{q})$

It is possible to write down the interference factor for each of these structures in two different forms by substituting the expressions for σ_x , σ_y and σ_z in 2(a) and (b). Since the expressions so obtained for $S_2(\mathbf{q})$ and $S_3(\mathbf{q})$ consist of scalar terms, they could be reduced to convenient forms. For instance, the expression for $S_2(\mathbf{q})$ in the case of hcp structure is reduced to (A1) when the terms with common denominators are collected together while that for $S_3(\mathbf{q})$ is reduced to (A2) when the products of the trigonometric functions are transformed into their sums. On the other hand, the expression for $S_2(\mathbf{q})$ in the case of ccp structure goes over to (A3) when the sums of the trigonometric functions are transformed into their products whereas the reverse transformation reduces that for $S_3(\mathbf{q})$ to (A4). Hence these expressions which are collected together in appendix A are just two of the several alternative (but equivalent) ways of writing down the interference factor. However, the contributions from the rhombic faces which bisect the basis vectors in both structures and those from the trapezoidal or parallelogram faces of the atomic polyhedron are not shown here separately as the former could easily

be distinguished from the latter in all expressions for $S(\mathbf{q})$. Besides, these expressions for ccp structure with $t = 1.633$ are reduced to the corresponding expressions for fcc structure (*viz* A1 and A2 in I) by a co-ordinate axes transformation which orients the z , x and y axes of the former along the $[111]$, $[\bar{1}10]$ and $[\bar{1}\bar{1}2]$ directions of the latter. On the contrary, there is no way of transforming the former, at any value of t , to those of hcp structure which are invariably complex, mainly because of the differences in their atomic arrangements.

It could, however, be shown that the apparently different expressions for $S_2(\mathbf{q}, t)$ and $S_3(\mathbf{q}, t)$ reduce to the same expressions along the principal symmetry directions of the crystal, provided their singularity is overcome by means of L'Hospital's rule. These expressions for the interference factor along $[\zeta 00]$, $[0\zeta 0]$ and $[00\zeta]$ directions denoted respectively by (B1), (B2) and (B3) in the case of hcp structure and by (B4), (B5) and (B6) in the case of ccp structure, where ζ is the appropriate reduced wavevector, are included in appendix B. It may be observed that the corresponding expressions for the two structures are identical except for the imaginary part of $S(\zeta, t)$ in (B2) and in the limit of $t \rightarrow 1.633$, they go over respectively, to those of the fcc structure along $[\zeta\zeta 0]$, $[\zeta\zeta 2\zeta]$ and $[\zeta\zeta\zeta]$ directions. In addition, each of these expressions tends to unity (while the imaginary part in B2 tends to zero) in the limit of $\zeta \rightarrow 0$ and becomes zero when ζ corresponds to a reciprocal lattice vector, $\mathbf{g} \neq 0$. They have been plotted as a function of ζ in the case of hcp and ccp structures with $t = 1.633$ in figures 2(a) and (b) respectively along $[\zeta 00]$, $[00\zeta]$ and $[0\zeta 0]$ directions as well as along a non-symmetry direction, $[\zeta\zeta\zeta]$. Numerical values of the interference factor, $G(qr_s)$ which approximates the atomic polyhedron by an ellipsoid of equivalent volume, calculated from the expression (C1) in appendix C have also been plotted in these figures to facilitate their comparison with the corresponding values of $S(\zeta, t)$.

4. Discussion

It is obvious from figures 2(a) and (b) that the interference factor, $S(\zeta, t)$ varies significantly with the direction at any value of t and its real as well as imaginary parts go through zero at values of ζ corresponding to $\mathbf{g} \neq 0$ whereas $G(qr_s)$ does not. Further, the numerical values of $G(qr_s)$ for hcp and ccp structures which are insensitive to the shapes of their atomic polyhedra, are identical at all wavevectors. On the other hand, the basis atoms of hcp structure destroy the centre of symmetry of its polyhedron and hence the expressions for $S(\zeta, t)$ become complex while those of ccp structure, referred to orthorhombic co-ordinate axes, do not. Nevertheless, the imaginary parts of the former are reduced to zero and the corresponding expressions for $S(\zeta, t)$ become equal along $[\zeta 00]$, $[00\zeta]$ and $[\zeta\zeta\zeta]$ directions mainly because the atomic arrangements of both structures are identical along these directions, whereas the differences along other directions manifest themselves as imaginary parts of $S(\zeta, t)$. Since the surface of the ellipsoid of equivalent volume does not match with that of the atomic polyhedron in any direction and the former lies outside the latter along $[\zeta 00]$, $[0\zeta 0]$, $[00\zeta]$ and $[\zeta\zeta\zeta]$ directions, the values of $G(qr_s)$ are higher than those of $S(\zeta, t)$, but the proximity of these surfaces at $t = 1.633$ gives rise to least differences between the two along $[\zeta 00]$ and $[\zeta\zeta\zeta]$ directions. However, the numerical values of t associated with the hcp arrangement invariably deviate from its unique value, 1.633 associated with the ccp arrangement. As a consequence, interference factors of the former differ from those of

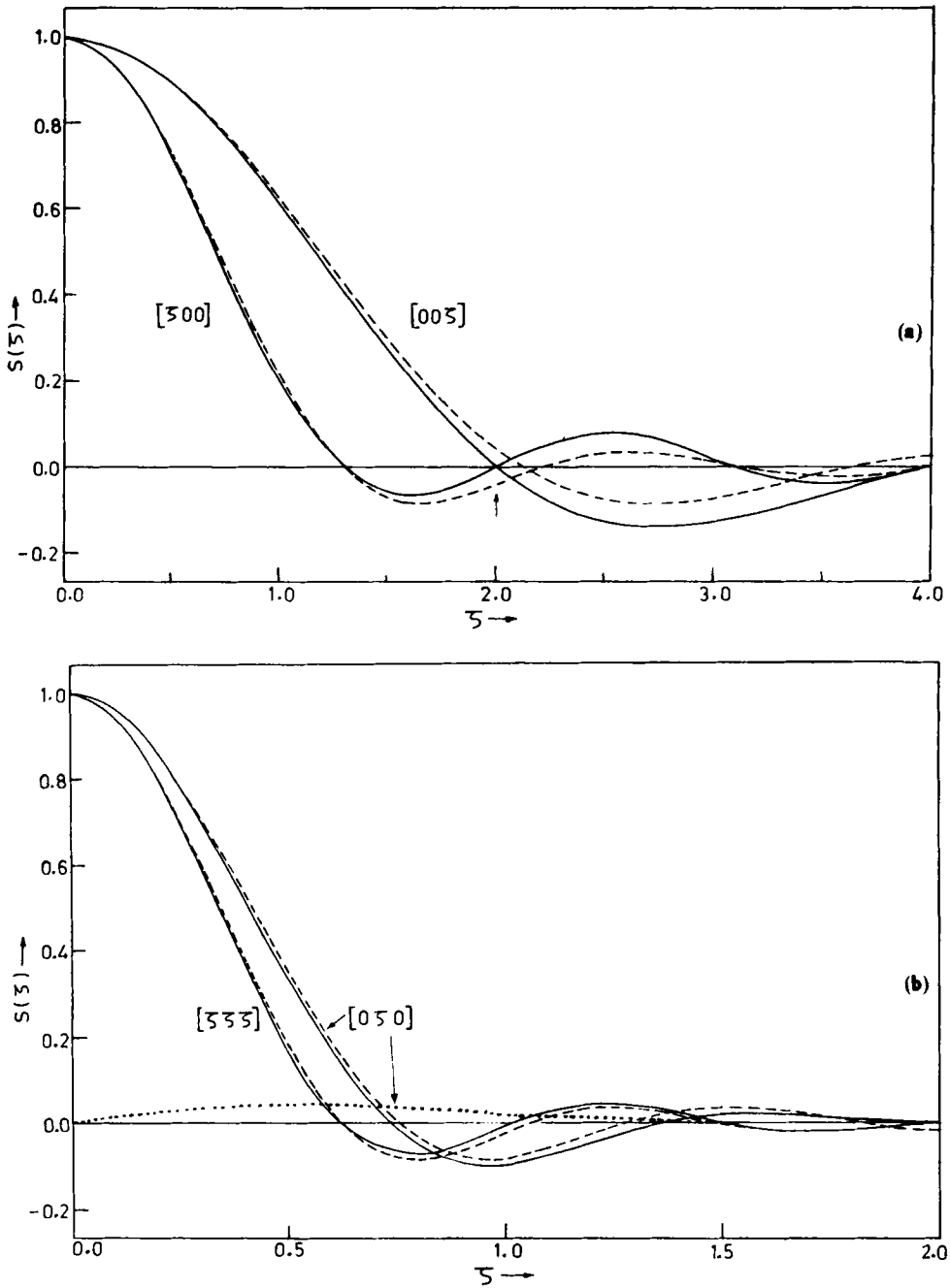


Figure 2. ζ -dependence of interference factors in the case of hcp and ccp structures along (a) $[100]$, $[001]$ directions and (b) $[111]$, $[010]$ directions (see appendix for appropriate expressions): (—), $S(\zeta)$; (---) $G(q, r_s)$; (· · ·), Imaginary part of $S(\zeta)$ for hcp structure. Other values are identical for both structures. The arrow in (a) indicates that $S(\zeta)$ passes through zero whereas $G(qr_s)$ does not, at a nonzero reciprocal lattice vector.

the latter at all wavevectors and the differences between $S(\zeta, t)$ and $G(qr_s)$ of hcp structure manifest themselves even at small values of ζ in all directions.

It was shown in I that the Wigner-Seitz approximation leads to an erroneous evaluation of the contributions from umklapp processes to the thermal and electrical properties of metals and is not consistent with the symmetry requirements of the lattice. Besides, the acoustical and optical modes of vibration of a diatomic lattice are associated, respectively with the 'in-phase' and 'out-of-phase' motion of the basis atoms. Different amplitudes of thermal motion of lattice and basis atoms make it all the more important to separate the latter contributions to the interference factor from the former contributions. Since there was no means of distinguishing these different contributions to $G(qr_s)$, several authors (Gupta and Dayal 1965; Sharan and Bajpai 1970; Bose *et al* 1973, Upadhyaya and Verma 1973; Saxena and Rathore 1984) assumed wrongly that the contributions from electron-ion interactions to the optical modes are the same as those to the acoustical modes and neither of these branches conforms to the translational symmetry of the lattice. It should therefore be apparent from this discussion that the correct evaluation of the contributions from normal and umklapp processes to different modes of vibration in a hexagonal lattice requires the exact evaluation of the interference factor over the actual shape of its atomic polyhedron so that it is expressed as a sum of the contributions from rhombic planes (bisecting the basis vectors) and trapezoidal planes (bisecting the lattice vectors). Further, the co-ordinate axes transformation which transforms the triatomic ocp structure, referred to the orthorhombic co-ordinate axes, to the monoatomic ocp structure referred to cubic co-ordinate axes (see §3.3) has been exploited to identify the correct set of reciprocal lattice vectors as well as to ensure that the method of evaluation of the electron-ion interactions in a polyatomic structure, described elsewhere (Ramamurthy 1985) is free from any mathematical or numerical errors.

5. Conclusions

The symmetry of the atomic polyhedra of hcp and ccp structures simplifies considerably the exact evaluation of the electron-ion matrix elements over their actual shape and facilitates the separation of the lattice atom contributions from the basis atom contributions to the interference factors, $S(\mathbf{q}, t)$. The imaginary part of $S(\mathbf{q}, t)$ for hcp structure reduces to zero and hence the two close packed structures have the same expressions for $S(\mathbf{q}, t)$ in certain directions, but they differ from each other in other directions as well as at different values of t . Since the lattice and basis atom contributions are inseparable in $G(qr_s)$, Wigner-Seitz approximation is not valid for a diatomic lattice and exact expressions for $S(\mathbf{q}, t)$ are required for a proper evaluation of thermal and electrical properties of hcp metals and to satisfy the symmetry requirements of the lattice.

Acknowledgements

The author is grateful to Dr S B Rajendraprasad and Mr A Thayumanavan for their assistance in computation and to Dr D Ranganathan for valuable discussions.

Appendix A. Expressions for $S(\mathbf{q}, t)$: general direction

(a) *hcp structure*

$$\begin{aligned}
 S_2(\mathbf{q}, t) = & \frac{2\alpha}{(u+v+\omega)} \left(\left[\frac{\exp(i\beta\omega)}{i\omega} \left\{ \frac{\sin u \sin(v'+\alpha\omega)}{(v'+\alpha\omega)} \right. \right. \right. \\
 & + \frac{(1+t_1) \sin\left(\frac{u+t_1v}{2}\right) \sin\left(\frac{u-v'+2\alpha\omega}{2}\right)}{(u-v'+2\alpha\omega)} \\
 & \left. \left. \left. + \frac{(1-t_1) \sin\left(\frac{u-t_1v}{2}\right) \sin\left(\frac{u+v'-2\alpha\omega}{2}\right)}{(u+v'-2\alpha\omega)} \right\} \right] \right. \\
 & \left. + \text{a term with } \omega \text{ and } -\omega \text{ interchanged} \right] + \left[2(2+s) \right. \\
 & \left. \left\{ \frac{\exp[i(2v'+t\omega)/2] \sin\left(\frac{u+v'-2\alpha\omega}{2}\right) \sin\left(\frac{u-v'+2\alpha\omega}{2}\right)}{i[u^2-(v'-2\alpha\omega)^2]} \right\} \right. \\
 & \left. + 2(2-s) \{ \text{a term with } \omega \text{ and } -\omega \text{ interchanged} \} \right. \\
 & + (t_1-1+s) \left\{ \frac{\exp[i(u-v'+t\omega)/2] \sin\left(\frac{u+v'-2\alpha\omega}{2}\right) \sin(v'+\omega)}{i(u+v'-2\alpha\omega)(v'+\alpha\omega)} \right\} \\
 & + (s-t_1-1) \{ \text{a term with } u \text{ and } -u \text{ interchanged} \} \\
 & + (t_1-1-s) \{ \text{a term with } \omega \text{ and } -\omega \text{ interchanged} \} \\
 & \left. - (t_1+1+s) \{ \text{a term with } u, \omega \text{ and } -u, -\omega \text{ interchanged} \} \right] / s, \quad (\text{A1})
 \end{aligned}$$

$$\begin{aligned}
 S_3(\mathbf{q}, t) = & \frac{\alpha}{(u^2+v^2+\omega^2)} \left(\left[\frac{\exp(i\beta\omega)}{i\omega} \left\{ u \left(\frac{\cos(u-v'-\alpha\omega) - \cos(u+v'+\alpha\omega)}{(v'+\alpha\omega)} \right) \right. \right. \right. \\
 & + (u+t_1v) \left(\frac{\cos(2v'-\alpha\omega) - \cos(u+v'+\alpha\omega)}{(u-v'+2\alpha\omega)} \right) \\
 & \left. \left. \left. + (u-t_1v) \left(\frac{\cos(2v'-\alpha\omega) - \cos(u-v'-\alpha\omega)}{(u+v'-2\alpha\omega)} \right) \right\} \right] \right. \\
 & \left. + \text{a term with } \omega \text{ and } -\omega \text{ interchanged} \right] \\
 & + \left[\left\{ \frac{2(2v'+t\omega) \exp[i(2v'+t\omega)/2]}{i[u^2-(v'-2\alpha\omega)^2]} (\cos[v'-2\alpha\omega] - \cos u) \right. \right. \\
 & \left. \left. + \text{a term with } \omega \text{ and } -\omega \text{ interchanged} \right\} \right]
 \end{aligned}$$

$$\begin{aligned}
 & + \left\{ \frac{(u-v'+t\omega) \exp [i(u-v'+t\omega)/2]}{i(u+v'-2\alpha\omega)(v'+\alpha\omega)} \left(\cos \left[\frac{u-v'-4\alpha\omega}{2} \right] - \cos \left[\frac{u+t_1v}{2} \right] \right) \right. \\
 & + \text{a term with } u \text{ and } -u \text{ interchanged} \\
 & + \text{a term with } \omega \text{ and } -\omega \text{ interchanged} \\
 & \left. + \text{a term with } u, \omega \text{ and } -u, -\omega \text{ interchanged} \right\} \Big/ t \quad (A2)
 \end{aligned}$$

(b) *ccp structure*

$$\begin{aligned}
 S_2(\mathbf{q}, t) = & \frac{4\alpha}{(u+v+\omega)} \left(\frac{\sin(\beta\omega)}{\omega} \left\{ \frac{\sin u \sin(v'+\alpha\omega)}{(v'+\alpha\omega)} \right. \right. \\
 & + \frac{(1+t_1) \sin \left(\frac{u+t_1v}{2} \right) \sin \left(\frac{u-v'+2\alpha\omega}{2} \right)}{(u-v'+2\alpha\omega)} \\
 & \left. \left. + \frac{(1-t_1) \sin \left(\frac{u-t_1v}{2} \right) \sin \left(\frac{u+v'-2\alpha\omega}{2} \right)}{(u+v'-2\alpha\omega)} \right\} \right) \\
 & + \left[\frac{(t_1-1+s) \sin \left(\frac{u-v'+t\omega}{2} \right) \sin \left(\frac{u+v'-2\alpha\omega}{2} \right) \sin(v'+\alpha\omega)}{(u+v'-2\alpha\omega)(v'+\alpha\omega)} \right. \\
 & + (s-t_1-1) \text{ (a term with } u \text{ and } -u \text{ interchanged)} \\
 & \left. + (2+s) \text{ (a term with } (u)-(v') \text{ and } 2v' \text{ interchanged)} \right] \Big/ s \quad (A3)
 \end{aligned}$$

$$\begin{aligned}
 S_3(\mathbf{q}, t) = & \frac{\alpha}{(u^2+v^2+\omega^2)} \\
 & \left(u \left\{ \frac{\sin(u+v'-\delta\omega) - \sin(u+v'+t\omega/2) + \sin(u-v'+\delta\omega) - \sin(u-v'-t\omega/2)}{\omega(v'+\alpha\omega)} \right\} \right. \\
 & + \left[(u+t_1v) \left\{ \frac{\sin(2v'+\delta\omega) - \sin(2v'-t\omega/2) + \sin(u+v'-\delta\omega) - \sin(u+v'+t\omega/2)}{\omega(u-v'+2\alpha\omega)} \right\} \right. \\
 & + \text{a term with } u \text{ and } -u \text{ interchanged} \\
 & + \left[(u-v'+t\omega) \left\{ \frac{\sin(u-v'+\delta\omega) + \sin[(t-\delta)\omega] - \sin(u+v'+t\omega/2) + \sin(2v'-t\omega/2)}{(u+v'-2\alpha\omega)(v'+\alpha\omega)} \right\} \right. \\
 & + \text{a term with } u \text{ and } -u \text{ interchanged} \\
 & \left. \left. + \text{a term with } (u)-(v') \text{ and } 2v' \text{ interchanged} \right] \Big/ t \quad (A4)
 \end{aligned}$$

where $u = q_x a$, $v = q_y a$, $\omega = q_z a$, $v' = v/t_1$, $\alpha = 1/3t$,

$$\beta = (t/2 - \alpha) \quad \text{and} \quad \delta = (\beta - \alpha).$$

Appendix B. Expressions for $S(\mathbf{q}, t)$: symmetry directions

(a) *hcp structure*

[$\zeta 00$] direction

$$S(\zeta, t) = \frac{\sin(\pi\zeta/2)}{(\pi\zeta/2)} \left[\left(\frac{2}{3} - \frac{4}{9t^2} \right) \cos(\pi\zeta/2) + \left(\frac{1}{3} + \frac{4}{9t^2} \right) \frac{\sin(\pi\zeta/2)}{(\pi\zeta/2)} \right], \quad (\text{B1})$$

[$0\zeta 0$] direction

$$S(\zeta, t) = \frac{\sin(\pi\zeta/2)}{(\pi\zeta/2)} \left[\left(1 - \frac{2}{3t^2} \right) \frac{\sin(3\pi\zeta/2)}{(3\pi\zeta/2)} + \frac{2}{3t^2} \frac{\sin(\pi\zeta) \sin(\pi\zeta/2)}{(\pi\zeta)(\pi\zeta/2)} + i \frac{2}{9t^2} \frac{\sin^3(\pi\zeta/2)}{(\pi\zeta/2)^2} \right], \quad (\text{B2})$$

[00ζ] direction

$$S(\zeta, t) = 18t^4 \sin(\pi\zeta/2) \sin^2(\pi\zeta/3t^2)/(\pi\zeta)^3 \quad (\text{B3})$$

(b) *ccp structure*

[$\zeta 00$] direction

$$S(\zeta, t) = \frac{\sin(\pi\zeta/2)}{(\pi\zeta/2)} \left[\left(\frac{2}{3} - \frac{4}{9t^2} \right) \cos(\pi\zeta/2) + \left(\frac{1}{3} + \frac{4}{9t^2} \right) \frac{\sin(\pi\zeta/2)}{(\pi\zeta/2)} \right], \quad (\text{B4})$$

[$0\zeta 0$] direction

$$S(\zeta, t) = \frac{\sin(\pi\zeta/2)}{(\pi\zeta/2)} \left[\left(1 - \frac{2}{3t^2} \right) \frac{\sin(3\pi\zeta/2)}{(3\pi\zeta/2)} + \frac{2}{3t^2} \frac{\sin(\pi\zeta) \sin(\pi\zeta/2)}{(\pi\zeta)(\pi\zeta/2)} \right], \quad (\text{B5})$$

[00ζ] direction

$$S(\zeta, t) = 18t^4 \sin(\pi\zeta/2) \sin^2(\pi\zeta/3t^2)/(\pi\zeta)^3, \quad (\text{B6})$$

where the reduced wavevector, $\zeta = q_x a/\pi$, $q_y a/\pi \sqrt{3}$ and $q_z c/\pi$ along x , y and z directions, respectively.

Appendix C. Expression for $G(qr_s)$

$$G(qr_s) = 3 [\sin(qr_s) - (qr_s) \cos(qr_s)] / (qr_s)^3, \quad (\text{C1})$$

where

$$qr_s = \left(\frac{t}{2\pi} \right)^{1/3} [3(u^2 + v^2 + \omega^2)]^{1/2}.$$

References

Ashokkumar 1973 *Noncentral interactions in metals*, Ph.D. Thesis, Indian Institute of Technology, Delhi, p. 49

- Bose G, Gupta H C and Tripathi B B 1973 *Phys. Lett.* **A43** 365
Bross H and Bohn B 1967 *Phys. Status Solidi* **20** 277
Gupta R P and Dayal B 1965 *Phys. Status Solidi* **8** 115
Ramamurthy V 1978 *Pramana* **11** 233
Ramamurthy V 1979 *Pramana* **13** 373
Ramamurthy V and Singh K K 1978 *Phys. Status Solidi* **B85** 761
Sharan B and Bajpai R P 1970 *J. Phys. Soc. Jpn.* **29** 46
Sharan B, Ashokkumar and Neelakandan K 1972 *Solid State Commun.* **11** 1223
Sharan B, Ashokkumar and Neelakandan K 1973 *J. Phys.* **F3** 1308
Saxena H C and Rathore R P S 1984 *Phys. Status Solidi* **B122** K 119
Upadhyaya J C and Verma M P 1973 *Phys. Rev.* **B8** 593